Supporting Information

Preparation of [Ag([18]aneS$_4$O$_2$)]PF$_6$

To a solution of [18]aneS$_4$O$_2$ (49.2 mg, 0.15 mmol) in CH_2Cl_2 (5 mL) was added slowly a solution of $AgPF_6$ (38 mg, 0.15 mml) in CH_3OH (3 mL). The reaction mixture was stirred at room temperature for 30 mins and diethyl ether (100 mL) added to afford a white precipitate. The solid was collected and dissolved in CH_3CN (1 mL), which was layered with diethyl ether in a thin tube at -20^{o}C to yield [Ag([18]aneS$_4$O$_2$)]PF$_6$·CH_3CN as colourless crystals. Yield 74.6mg, 80%. Anal. Calcd for $C_{14}H_{27}S_4O_2NPF_6Ag$: C, 27.01; H, 4.37; N, 2.25. Found: C, 26.85; H, 4.22; N, 2.17. IR (KBr, cm^{-1}): 2957 (w), 2930 (w), 2919 (w), 2889 (m), 2859 (m), 2786 (w), 2254 (w), 1477 (w), 1421 (m), 1394 (w), 1358 (w), 1285 (w), 1204 (m), 1136 (m), 1110 (s), 1045 (m), 1005 (w), 852-831 (vs, broad), 721 (m), 651 (w), 560 (s). M.S. (ES): *m*/*z* 437 for [Ag([18]aneS$_4$O$_2$)]$^+$ with correct isotopic distribution.

Electrochemical generation and electrocrystallisation of [Ag([18]aneS$_4$O$_2$)](PF$_6$)$_2$

In an optically transparent electrochemical (OTE) quartz cell (40 × 10 × 0.5 mm^3) equipped with a Pt/Rh gauze working electrode, a Pt wire secondary electrode and a saturated calomel electrode (Fig. S1), the Ag(I) complex [Ag([18]aneS$_4$O$_2$)]PF$_6$·CH_3CN (2 mg, 3.2 × 10^{-3} mmol) in CH_2Cl_2 (1.5 mL) containing NBu_4PF_6 (0.4 M) was oxidised by controlled potential electrolysis at +1.12 V *vs*. Fc^+/Fc at -20^{o}C under N_2. Blue needle crystals suitable for X-ray crystallographic analysis were deposited on the surface of working electrode over 1 h. Yield 2.4 mg, 92%. Uv-vis (in CH_3CN) [λ_{max}(ε_{max})]: 574 nm (3083 L mol^{-1} cm^{-1}, broad).

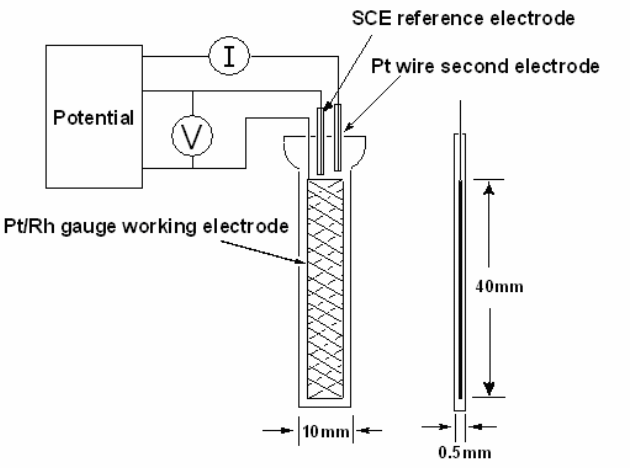

Figure S1: View of electrocrystallisation system

X-ray single crystal structure determination of [Ag([18]aneS$_4$O$_2$)]PF$_6$·CH$_3$CN

A colourless lath crystal (0.43 × 0.10 × 0.03 mm^3) was coated with Fomblin perfluoropolyether (YR-1800; Lancaster Synthesis) and mounted on a glass fibre for data collection using the Bruker SMART 1000 CCD area detector in Nottingham. The wavelength used was 0.71073 Å.

Crystal data $C_{14}H_{27}NO_2S_4PF_6Ag$, M = 622.45, Orthorhombic, a = 21.0076(4), b = 17.5973(6), c = 12.5610(7) Å, V = 4643.5(3) Å^3, T = 150(2) K, space group $Pna2_1$, Z = 8, D_c = 1.781 g/cm^3, 11085 unique reflections (R_{int} = 0.0282). One carbon atom in macrocycle ring was disordered to two anisotropic atoms of C29 and C29', but attempts to develop a disorder model for its adjacent carbon atom of C30 failed. The four hydrogen atoms on these two carbon atoms were not included in the refinement model. In addition, five fluorine atoms in one PF_6^- anion were disordered to two anisotropic atoms, but the sixth fluorine was refined as ordered. All non-hydrogen atoms were refined with anisotropic displacement parameters except for those of disordered atoms. Hydrogen atoms were located by geometrically calculation except for the hydrogen atoms on C29 and C29' and C30. Application of disorder modelling and distance restraints led to stable refinement. Final $R_1[F > 2\sigma(F)]$ = 0.030, wR_2 (all data) = 0.0705.

X-ray single crystal structure determination of [Ag([18]aneS$_4$O$_2$)](PF$_6$)$_2$·CH$_2$Cl$_2$

A blue needle crystal (0.13 × 0.015 × 0.015 mm^3) was coated with Fomblin perfluoropolyether (YR-1800; Lancaster Synthesis) and mounted on a glass fibre for data collection using the Bruker SMART APEXII diffractometer on Station 16.2smx of the Daresbury Synchrotron Radiation Source. The wavelength used was 0.7848 Å.

Crystal data $C_{13}H_{26}O_2S_4Cl_2P_2F_{12}Ag$, M = 811.29, monoclinic, a = 11.190(2), b = 10.510(2), c = 22.990(5) Å, β = 91.00(3), V = 2703.4(9) Å^3, T = 150(2) K, space group $P2_1/n$ (*alt.* $P2_1/c$, no. 14), Z = 4, D_c = 1.993 g/cm^3, 4733 unique reflections (R_{int} = 0.177). Data were truncated to 2θ = 50° due to lack of diffraction intensity beyond this limit. Atoms C3, C5, C6, C8, C12, C14, C15, C17 and C18 in the macrocyclic ring and the two chlorine atoms (Cl1, Cl2) of the CH_2Cl_2 solvent molecule all exhibited strongly elongated ellipsoids and their U_{eq} values were all much higher than those of adjacent atoms. Therefore, each of these atoms was modelled as disordered over two half-occupied positions, resulting in final U_{eq} values of less than 0.10 Å^2. The H atoms of the CH_2Cl_2 were not included in the model. Distance restraints were applied to all macrocyclic C–C, C–O and C–S bonds, to the P–F bonds in the PF_6 anion and to the C–Cl bonds in the CH_2Cl_2 solvent molecule. Application of disorder modelling and distance restraints led to stable refinement. Final $R_1[F > 4\sigma(F)]$ = 0.0944, wR_2 (all data) = 0.251.

Selected bond lengths (Å) and angles (°) of $[Ag([18]aneS_4O_2)]^+$

Ag1···O1	3.092(3)	S4-Ag1-S7	85.44(4)
Ag1-S4	2.574(6)	S4-Ag1-S13	113.39(4)
Ag1-S7	2.609(4)	S4-Ag1-S16	132.99(3)
Ag1···O10	3.022(3)	S7-Ag1-S13	135.30(3)
Ag1-S13	2.574(5)	S7-Ag1-S16	111.31(4)
Ag1-S16	2.572(4)	S13-Ag1-S16	85.72(4)

Selected bond lengths (Å) and angles (°) of $[Ag([18]aneS_4O_2)]^{2+}$.

Ag1···O1	2.814(9)	S4-Ag1-S7	84.33(1)
Ag1-S4	2.487(4)	S4-Ag1-S13	168.18(2)
Ag1-S7	2.537(4)	S4-Ag1-S16	93.51(14)
Ag1···O10	2.797(10)	S7-Ag1-S13	94.88(13)
Ag1-S13	2.501(4)	S7-Ag1-S16	168.01(15)
Ag1-S16	2.518(4)	S13-Ag1-S16	84.81(14)

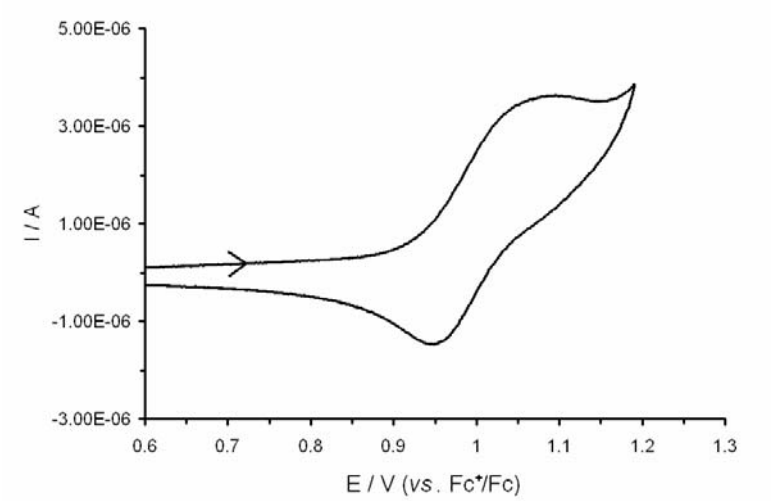

Figure S3: The cyclic voltammogram of $[Ag([18]aneS_4O_2)]PF_6$ in CH_2Cl_2 (0.4 M NBu_4PF_6) at a scan rate of 100 mV s^{-1} (253 K).

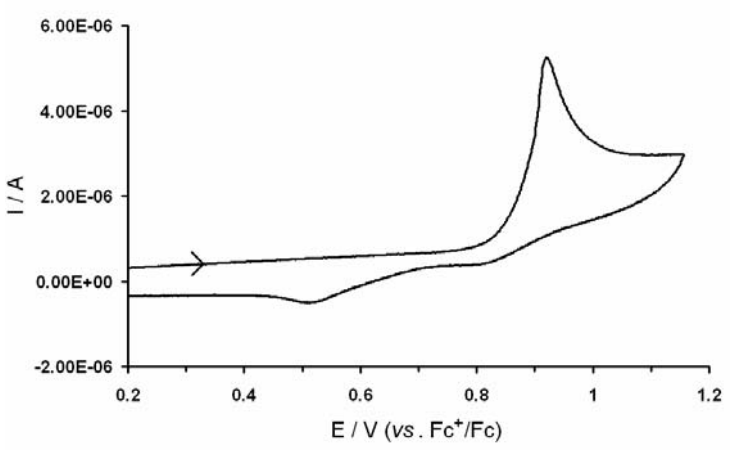

Figure S4: Cyclic voltammogram of $[Ag([18]aneS_6)]PF_6$ in CH_2Cl_2 containing NBu_4PF_6 (0.4 M) at 253 K at a scan rate of 100 mV/s.

EPR Spectroscopy and Simulation

The Q- and S-band frozen EPR spectra of $[Ag([18]aneS_4O_2)]^{2+}$ specie was recorded at the Manchester EPR centre on a Bruker ESP 300E spectrometer. The X-band fluid and frozen spectra were recorded on a Bruker EMX EPR spectrometer. All the frozen solutions were kept cooled at a temperature of *ca.*125 K by an Oxford cooling device throughout the experiments. All the EPR simulations of Ag(II) spectra were performed using Simfornia package[1] in Nottingham.

EPR theoretical calculation

The axial EPR spectra of $[Ag([18]aneS_4O_2)]^{2+}$ are consistent with the approximate square-planar molecular structure determined by X-ray crystallography. Thus, the *z*-axis was defined as being perpendicular to the S_4 plane with $g_\parallel$ and $A_\parallel$ lying along this axis, with the *x*-axis defined as pointing along the bisector of the S(4)-Ag(1)-S(16) angle. Thus, crystal field theory predicts a $4d_{xy}$-based SOMO in $[Ag([18]aneS_4O_2)]^{2+}$ consistent with the observed $g_\parallel > g_\perp > g_e$ pattern in the EPR spectra of the complex. For this case perturbation theory, where $g_{11} = g_{22} = g_{xx} = g_{yy}$, $g_{33} = g_{zz}$, $A_{11} = A_{22} = A_{xx} = A_{yy}$ and $A_{33} = A_{zz}$, gives for Δg_{ii} and A_{ii} ($i = x, y, z$):[2]

$$\Delta g_{xx} = 2\lambda/\delta_{yz} = g_{xx} - g_e \quad (1)$$

$$\Delta g_{yy} = 2\lambda/\delta_{xz} = g_{yy} - g_e \quad (2)$$

$$\Delta g_{zz} = 8\lambda/\delta_{x^2-y^2} = g_{zz} - g_e \quad (3)$$

$$A_{xx} = A_s + P_d[2\alpha^2/7 + \Delta g_{xx} - 3\Delta g_{yy}/14] \quad (4)$$

$$A_{yy} = A_s + P_d[2\alpha^2/7 + \Delta g_{yy} - 3\Delta g_{xx}/14] \quad (5)$$

$$A_{zz} = A_s + P_d[-4\alpha^2/7 + \Delta g_{zz} + 3(\Delta g_{xx} + \Delta g_{yy})/14] \quad (6)$$

where g_e is the *g*-value of the free electron 2.00232, λ is the spin-orbit coupling constant for Ag(II), δ_{ij} is the weighted average energy difference between the ground and excited states, α is the LCAO coefficient of the Ag ($4d_{xy}$) orbital in the SOMO, A_s is the isotropic Fermi contact term and P_d is the electron-nuclear dipolar coupling parameter for Ag(II), which was calculated as -74.7×10^{-4} cm^{-1} using Rieger's methodology.[3] A combination of equations (1) - (6) gives:

$$A_{zz} = \langle A \rangle + P_d[-4\alpha^2/7 + 2\Delta g_{zz}/3 - 5(\Delta g_{xx} + \Delta g_{yy})/42] \quad (7) \quad \text{where } \langle A \rangle = (A_{xx} + A_{yy} + A_{zz})/3$$

Solution of (7) with the simulated *g* and *A*-values from the multi-frequency EPR spectra gave $\alpha^2 = 22.7\%$ with $A_{zz} \equiv A_\parallel$ and $g_{zz} = g_\parallel$. Negative *A*-values gave invalid negative values for α^2.

Thus, the contribution of 4d_{xy} metal orbital to the SOMO is 22.7% as determined by multi-frequency EPR spectroscopy.

DFT Calculations

The calculations were performed using the Amsterdam Density Functional (ADF) suite version 2005.01.[4,5] The unrestricted scalar relativistic DFT calculations employed a Slater type orbital (STO) triple-ζ-plus one polarization function basis set from the ZORA/TZP database of the ADF suite for all atoms. The cores were frozen up to and including 2*p* for S, 1*s* for C and O and 3*d* for Ag, respectively. The local density approximation (LDA) with the correlation potential due to Vosko *et al* [6] was used in all of the DFT calculations. Gradient corrections were performed using the functionals of Becke[7] and Perdew (BP).[8] A model of $[Ag[18]aneS_4O_2]^{2+}$ was constructed using geometrical data from the X-ray crystal structure and were optimised without any constraints on symmetry.

Geometry Optimised Coordinates for $[Ag([18]aneS_4O_2)]^{2+}$

Ag	0.00000	0.00000	0.00000
O	-1.66175	0.10182	-2.10540
C	-2.51445	-1.05672	-2.27095
H	-1.91800	-1.78777	-2.83225
H	-3.39576	-0.80516	-2.88208
C	-2.99032	-1.64541	-0.94216
H	-3.48173	-2.61713	-1.10267
H	-3.71624	-0.99619	-0.43302
S	-1.68910	-1.89962	0.34143
C	-0.67173	-3.29176	-0.32972
H	-1.26767	-4.20959	-0.21223
H	-0.47449	-3.12494	-1.39515
C	0.61455	-3.40609	0.48209
H	1.22460	-4.24725	0.12537
H	0.39926	-3.58764	1.54511
S	1.70508	-1.90851	0.52213
C	2.77611	-2.02353	-0.98394
H	3.68731	-1.49311	-0.67334
H	3.04895	-3.08150	-1.11288
C	2.20743	-1.45178	-2.28445
H	3.01394	-1.41090	-3.03401
H	1.40978	-2.09074	-2.68313
O	1.60477	-0.14587	-2.12520
C	2.41066	1.03560	-2.35206
H	1.76215	1.73700	-2.89248
H	3.26596	0.80027	-3.00538
C	2.93688	1.66271	-1.06012
H	3.39382	2.64277	-1.26420

H	3.70497	1.04251	-0.57750
S	1.69293	1.90851	0.28114
C	0.65154	3.30780	-0.33829
H	1.24462	4.22598	-0.21039
H	0.43677	3.16514	-1.40412
C	-0.62054	3.39857	0.49780
H	-1.23786	4.24713	0.17281
H	-0.38814	3.55369	1.56129
S	-1.70892	1.89962	0.51880
C	-2.77710	2.03043	-0.98898
H	-3.70605	1.53463	-0.67351
H	-3.01397	3.09483	-1.13259
C	-2.22611	1.42196	-2.28106
H	-3.03383	1.39492	-3.03024
H	-1.40918	2.02970	-2.68821

References

1. WINEPR SimFonia, version 1.25 and WINEPR System, version 2.11, 1996; Bruker Analytische Messtechnik GmbH, Germany.
2. P. H. Rieger, *Cood*. *Chem*. *Rev*., 1994, **135/136**, 203.
3. P. H. Rieger, *J*. *Magn*. *Reson*., 1997, **124**, 140.
4. C. F. Guerra, J. G. Snijders, G. te Velde and E. J. Baerends. *Theor*. *Chem*. *Acc*., 1998, **99**, 391.
5. G. te Velde, F. M. Bickelhaupt, S. J. A. van Gisbergen, C. F. Guerra, E. J. Baerends, J. G. Snijders and T. Ziegler. *J*. *Comput*. *Chem*., 2001, **22**, 931.
6. S. H. Vosko, L. Wilk and M. Nusair. *Can*. *J*. *Phys*., 1980, **58**, 1200.
7. A. D. Becke *Phys*. *Rev*. *A*, 1988**, 38**, 3098.
8. J. P. Perdew *Phys*. *Rev*. *B*, 1986**, 33**, 8822.